

---

**ABSTRACT**

This paper focus on 3D CFD analysis of an turbine blade cooling passage/duct in which the desired domain subjected to critical load i.e. static as well as dynamic load which is due turbine blade is operated at high temperature and pressure which results in thermal stress and alters the blade performance. In order to avoid clastatic failure of blade effective and efficient cooling techniques should be implemented which ultimately results in higher thermal efficiency and maximum power output. Extensive literature review is carried out in the field relating to turbine blade cooling. This work is concerned with the turbine surface blade internal duct cooling conventionally and with the help of coolant and heat transfer around the duct surface is been analysed and the performance is predicted with the help of Finite element volume tool ANSYS- Fluent, where simulation is being done. The goal is to carry out heat transfer coefficient at the turbine blade internal duct surface using different turbulent model as well as comparative case study is also been presented. The FEV results are validated with well published results in literature. In this research, which concluded that the V-shape 35-deg truncated ribs is the best as compared to the normal truncated and V-shape 35-deg continuous ribs for cooling the turbine blade after modification and analysis has been done. This investigation has been done the various solution analysis like; pressure drop, velocity, temperature, wall shear stress, heat transfer coefficient etc.

**KEYWORDS:** Turbine cooling blade duct, ANSYS CFD Fluent, Contineous rib, Truncated ribs etc.

---

**INTRODUCTION**

The various means of producing either thrust or power, the gas turbine engine is one of the most satisfactory. Its main advantages are: exceptional reliability, high thrust-to-weight ratio, and relative freedom of vibration. The work from a gas-turbine engine may be given either as torque in a shaft or as thrust in a jet. A gas-turbine consists of the following main parts: an inlet, a compressor, a combustor, a turbine and an exhaust, Fig. 1.1.



Figure 1.1: RM12, Gas Turbine

The inlet section may involve filters, valves and other arrangements to ensure a high quality of the flow. In flying applications, it is of importance to pay special consideration to the inlet as the ram-effect could boost the thrust significantly.

The pressure of the air is increased in the compressor, which is divided into several stages. There are two main types of compressors, radial – where the air enters axial but exits radially, or the more common axial compressor – where the flow is primarily axial. The rotation of the compressor increases the velocity of the air with the following diffusers converts the dynamic pressure (velocity) to static pressure. The compressor is connected to the turbine via a shaft running through the center of the engine. The operation of a gas-turbine relies on that the power gained from the turbine exceeds the power absorbed by the compressor. This is ensured by the addition of energy in the combustor, through igniting fuel in special purposed burners. The design and operation of these burners are vital for a high efficient engine if low emissions are to be achieved. The highly energetic gas from the combustor is expanded through a turbine, which drives the compressor in the front of the engine. After the turbine the gas still contains a significant amount of energy which can be extracted in various forms. In aircrafts the surplus energy is transformed into a high velocity jet in the nozzle which is the driving force that propels the vehicle through the air. The jet velocity and hence thrust could be further increased, through re-heating the gas in an afterburner. This is common in high performance aircraft, especially for military applications. For stationary, power generating gas turbines, the extra energy is converted into shaft-power in a power turbine.

Increasing Efficiency through Cooling Through the increased environmental awareness and higher fuel costs, there have lately been a strong strive towards enhanced efficiencies for all automotive propulsions. For gas turbines applications, especially in aircraft, not only the specific fuel consumption (SFC) is of importance but also the specific work output.

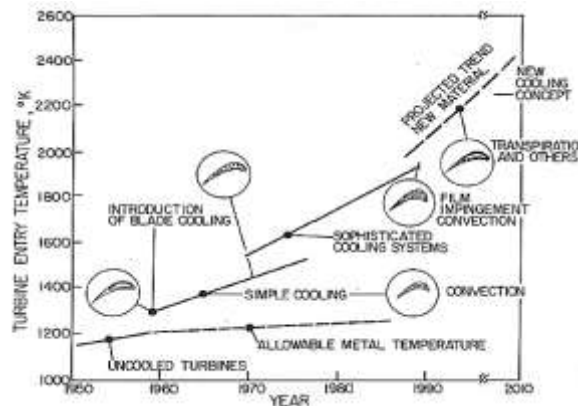


Figure 1.2 Evolution of Blade cooling

The former is equivalent to the inverse of the efficiency while the latter is a measure of the compactness of the power plant, ie. the effectiveness. The maximum theoretical efficiency of a gas turbine cycle is given by the Carnot efficiency as:

$$\eta = 1 - \frac{T_1}{T_3} \quad (1.1)$$

Where  $T_1$  the inlet temperature and  $T_3$  the turbine entry temperature (TET). Increasing yield, a direct improvement in the efficiency,  $\eta$ . The performance of practical cycles is however lower, due to pressure and mass flow losses, friction, components efficiency, non-ideal fluids etc. When these losses are taken into account, the efficiency of the simple gas turbine cycle becomes dependent not only of the temperature ratio, as in the Carnot process, but also the compressor pressure ratio. Thus the gas turbine industries are trying to reach both higher turbine temperatures as well as increased pressure ratio, to improve the efficiency and effectiveness of tomorrow's engines.

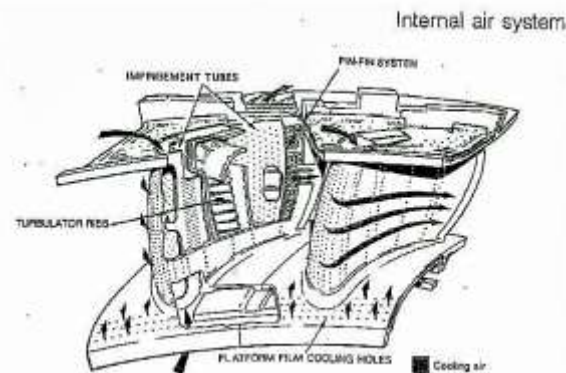


Figure 1.3: Cooling schemes, Inlet Guide Vane

Even though exotic materials are used for the most stressed environments, these have for the last decades been unable to withstand the demanded TET without yielding to the harsh environment. High strength material such as nickel and cobalt based super alloys, (eg. Inco 738 and Rene 220) will all weaken from increased temperatures, and since the loads in a rotating turbine are extremely high, the structure fails if not counter-measures are taken. The introduction of relatively cool gas from the compressor in well selected places in the turbine extends the engine endurance, and was in practice already during the Second World War. Figure 1.2 shows the increases in TET through the introduction of different cooling techniques. The highest temperatures loads are found at the exit of the combustor, and in the first turbine stage. A comprehensive cooling system are thus needed for the inlet guide vanes (IGV). A conceptual view of such as system is shown in Figure 1.3. These vanes employ both external cooling (film cooling), and internal cooling (convection- and impingement-cooling). The vanes are perforated by a number of small holes, through which compressed air is ejected. If correctly designed these holes will supply a cool protective air-film covering the vanes.

## LITERATURE SURVEY

Iacovides and Launder 1995, Presents review report on current capabilities for predicting flow in the cooling passages and cavities of jet engines. In report an attempts to show that progress is being made, particularly in respect to the flow in serpentine blade-cooling passages. The first essential in modeling such flows is to adopt a low Reynolds number model for the sub layer region. [1]

Srinath and Han 1997, Present Detailed Nusselt number distributions for a two-pass square channel with one ribbed wall. This wall of the channel is sprayed with thermo chromic liquid crystals, and a transient test is run to obtain the local heat transfer coefficients. Results are presented for Reynolds numbers ranging from 6000 to 60 000. [2]

Kadja and Bergelest 1997, Present a two-dimensional numerical model for the injection of a fluid through a slot into a free stream. The model is based on a finite-volume integration of the equations governing mass, momentum and heat transport. The solution accuracy was improved by using local grid refinement. The storage of variables was done in a collocated manner, thus allowing the reduction of storage requirements and a more accurate interfacing of the various sub-domains of the grid. [3]

Smith and Kempster 1999, Developed that facilitates the protective aluminide coating of the surface of internal cooling channels in superalloy turbine blades and vanes, without recourse to either reduced pressure or pressure pulsing. has been established that the internal surfaces have been coated with an aluminide layer that exhibits a good uniformity of thickness throughout. The coated internal cooling channel surfaces have additionally been shown to be clean and free from any extraneous material. [4]

Murata and Sadanari 2000, Investigate the effects of transverse ribs, the Coriolis force, and cross-sectional aspect ratios on turbulence; the large eddy simulation was performed changing the rotation number and the aspect ratio. The results reproduced the experimentally observed high heat transfer areas: in front of the rib on the rib-roughened walls and around the rib on the smooth side walls. In the rotating case, an interesting dissimilarity between the velocity and temperature fields was seen. [5]

A. Ooi, & M. Behnia 2002, Use eddy-viscosity type turbulence models for analyzing turbulent flows and heat transfer in complex passages for cooling turbine blade and there research presents numerical data from the calculation of the turbulent flow field and heat transfer in two-dimensional (2D) cavities and three-dimensional (3D)

ribbed ducts. It is found that heat transfer predictions obtained using the v2-f turbulence models for the 2D cavity are in good agreement with experimental data. [6]

## MATHEMATICAL MODELING

We develop the mathematical basis for a comprehensive general-purpose model of fluid flow and heat transfer from the basic principles of conservation of mass, momentum and energy. This leads to the governing equations of fluid flow and a discussion of the necessary auxiliary conditions – initial and boundary conditions. The main issues covered in this context are:

- Derivation of the system of partial differential equations (PDEs) that govern flows in Cartesian (x, y, z) coordinates
- Thermodynamic equations of state
- Newtonian model of viscous stresses leading to the Navier–Stokes equations
- Commonalities between the governing PDEs and the definition of the transport equation
- Integrated forms of the transport equation over a finite time interval and a finite control volume
- Classification of physical behaviours into three categories: elliptic, parabolic and hyperbolic
- Appropriate boundary conditions for each category
- Classification of fluid flows
- Auxiliary conditions for viscous fluid flows
- Problems with boundary condition specification in high Reynolds number and high Mach number flows.

### 3.1 Governing equations of fluid flow and heat transfer

The governing equations of fluid flow represent mathematical statements of the conservation laws of physics:

- The mass of a fluid is conserved
- The rate of change of momentum equals the sum of the forces on a fluid particle (Newton's second law)
- The rate of change of energy is equal to the sum of the rate of heat addition to and the rate of work done on a fluid particle (first law of thermodynamics)

The fluid will be regarded as a continuum. For the analysis of fluid flows at macroscopic length scales (say 1  $\mu\text{m}$  and larger) the molecular structure of matter and molecular motions may be ignored. We describe the behavior of the fluid in terms of macroscopic properties, such as velocity, pressure, density and temperature, and their space and time derivatives. These may be thought of as averages over suitably large numbers of molecules. A fluid particle or point in a fluid is then the smallest possible element of fluid whose macroscopic properties are not influenced by individual molecules.

We consider such a small element of fluid with sides  $\delta x$ ,  $\delta y$  and  $\delta z$  (Figure 3.1).

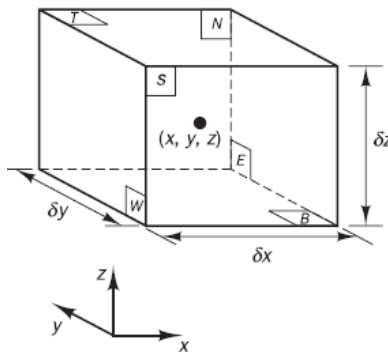


Figure 3.1 Fluid element for conservation laws

The six faces are labelled N, S, E, W, T and B, which stands for North, South, East, West, Top and Bottom. The positive directions along the coordinate axes are also given. The centre of the element is located at position (x, y, z). A systematic account of changes in the mass, momentum and energy of the fluid element due to fluid flow across its boundaries and, where appropriate, due to the action of sources inside the element, leads to the fluid flow equations. All fluid properties are functions of space and time so we would strictly need to write  $\rho(x, y, z, t)$ ,  $p(x, y, z, t)$ ,  $T(x, y, z, t)$  and  $u(x, y, z, t)$  for the density, pressure, temperature and the velocity vector respectively. To avoid unduly

cumbersome notation, we will not explicitly state the dependence on space co-ordinates and time. For instance, the density at the centre (x, y, z) of a fluid element at time t is denoted by  $\rho$  and the x-derivative of, say, pressure p at (x, y, z) and time t by  $\frac{\partial p}{\partial x}$ . This practice will also be followed for all other fluid properties. The element under consideration is so small that fluid properties at the faces can be expressed accurately enough by means of the first two terms of a Taylor series expansion. So, for example, the pressure at the W and E faces, which are both at a distance of  $1/2 \delta x$  from the element centre, can be expressed as

$$p - \frac{\partial p}{\partial x} \frac{1}{2} \delta x \quad \text{and} \quad p + \frac{\partial p}{\partial x} \frac{1}{2} \delta x \quad (3.1)$$

### 3.2 Mass conservation in three dimensions

The first step in the derivation of the mass conservation equation is to write down a mass balance for the fluid element: Rate of increase of flow of mass in fluid = Net rate of mass into element fluid element

The rate of increase of mass in the fluid element is

$$\frac{\partial}{\partial t} (\rho \delta x \delta y \delta z) = \frac{\partial \rho}{\partial t} \delta x \delta y \delta z \quad (3.2)$$

Next we need to account for the mass flow rate across a face of the element, which is given by the product of density, area and the velocity component normal to the face. From Figure 3.1 it can be seen that the net rate of flow of mass into the element across its boundaries is given by

$$\begin{aligned} & \left( \rho u - \frac{\partial(\rho u)}{\partial x} \frac{1}{2} \delta x \right) \delta y \delta z - \left( \rho u + \frac{\partial(\rho u)}{\partial x} \frac{1}{2} \delta x \right) \delta y \delta z \\ & + \left( \rho v - \frac{\partial(\rho v)}{\partial y} \frac{1}{2} \delta y \right) \delta x \delta z - \left( \rho v + \frac{\partial(\rho v)}{\partial y} \frac{1}{2} \delta y \right) \delta x \delta z \\ & + \left( \rho w - \frac{\partial(\rho w)}{\partial z} \frac{1}{2} \delta z \right) \delta x \delta y - \left( \rho w + \frac{\partial(\rho w)}{\partial z} \frac{1}{2} \delta z \right) \delta x \delta y \end{aligned} \quad (3.3)$$

Flows which are directed into the element produce an increase of mass in the element and get a positive sign and those flows that are leaving the element are given a negative sign.

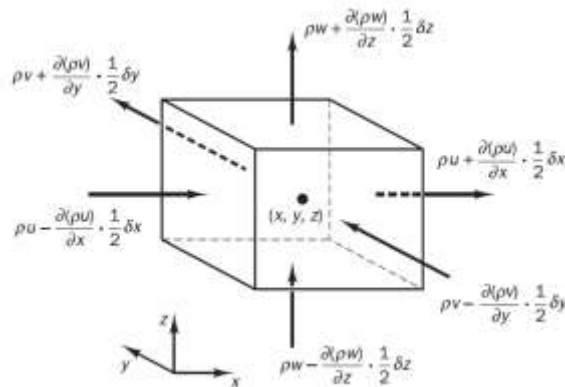


Figure 3.2 Mass flows in and out of fluid element

The rate of increase of mass inside the element (3.2) is now equated to the net rate of flow of mass into the element across its faces (3.3). All terms of the resulting mass balance are arranged on the left hand side of the equals sign and the expression is divided by the element volume  $\delta x \delta y \delta z$ . These yields

$$\frac{\partial \rho}{\partial t} + \frac{\partial(\rho u)}{\partial x} + \frac{\partial(\rho v)}{\partial y} + \frac{\partial(\rho w)}{\partial z} = 0 \quad (3.4)$$

or in more compact vector notation

$$\frac{\partial \rho}{\partial t} + \text{div}(\rho u) = 0 \quad (3.5)$$

Equation (3.5) is the unsteady, three-dimensional mass conservation or continuity equation at a point in a compressible fluid. The first term on the left hand side is the rate of change in time of the density (mass per unit volume). The second term describes the net flow of mass out of the element across its boundaries and is called the convective term. For an incompressible fluid (i.e. a liquid) the density  $\rho$  is constant and equation (3.4) becomes

$$\text{div } \mathbf{u} = 0 \quad (3.6)$$

or in longhand notation

$$\frac{\partial u}{\partial x} + \frac{\partial v}{\partial y} + \frac{\partial w}{\partial z} = 0 \quad (3.7)$$

## METHODOLOGY

The equation of motion of turbine blade internal duct surface is solved using FEV tool (ANSYS- Fluent) as the equation of motion for a internal duct is difficult to visualize therefore some FEV tool is the only solution method for analysing thermo physical characteristics of cavity.

The ANSYS 14.5 finite element program was used convection in differentially heated duct surface. For this purpose, the key points were first created and then line segments were formed. The lines were combined to create a surface. Finally, this surface is provided thickness model is made. We modeled turbine duct surface taking parameters from Gongnan. The blade surface was discretized into 1045 elements with 2318 nodes. The Internal duct boundary conditions can also be (provided in mesh section through naming the portion of modeled cavity i.e Inlet, Outlet, Heated region, Wall.

### 4.1 Model the Geometry

In this step model the geometry of product with the help of Creo parametric software. The turbine blade cooling ducts is not to designed completely and takes a part of duct system and design this product in Creo parametric as shown in below Figure 4..

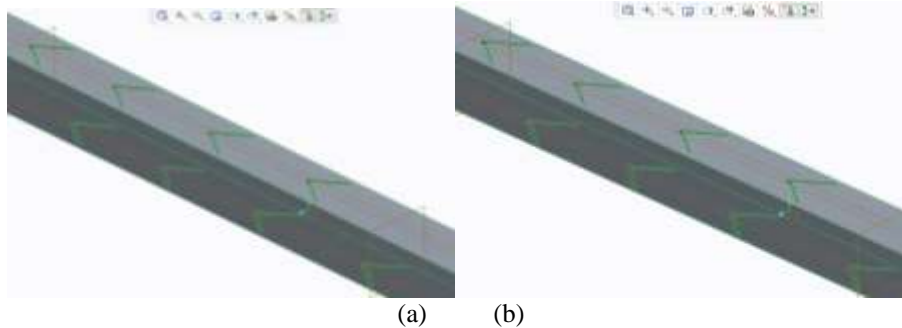


Figure 4.1 3D Model (V-shape 35-deg Truncated and Continuous ribs)

### 4.2 Generate Mesh

After modelling the product in Creo parametric import this file to Ansys fluent and generate mesh in model. In this process can uses unstructured meshing method as shown in Figure 4.2. Ansys Fluent uses unstructured meshes in order to reduce the amount of time you spend generating meshes, to simplify the geometry modeling and mesh generation process, to allow modeling of more complex geometries than you can handle with conventional, multi-block structured meshes, and to let you adapt the mesh to resolve the flow-field features.

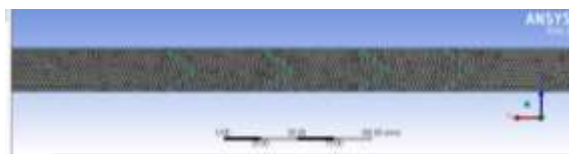


Figure 4.2 Mesh Model

### 4.3 Boundary Condition

In this step we can apply the boundary condition in duct like inlet, outlet, heated region & walls. In boundary condition give boundary condition name in mesh module such as Inlet, Outlet, Heated wall.



Figure 4.3: Boundary Condition

Table 1 Boundary Condition for Cooling Duct [11]

Boundary Condition	Value
<b>Inlet</b>	
Total Temperature	300 K
Total Pressure	342255 Pa
Turbulence Intensity	5 % $D_H$
Reynolds Number	20000
Air	Dry
Number of Ribs	8
pitch-to-height ratio	20
Rib height-to-hydraulic diameter ratio	0.0875
length-to-width of duct ratio, L/w	0.9
<b>Outlet</b>	
Static Pressure	204560Pa

The above Table 1 indicates that values of boundary condition of the cooling duct which is applied in cooling duct model.

## RESULT AND DISCUSSION

### 5.1 Validation

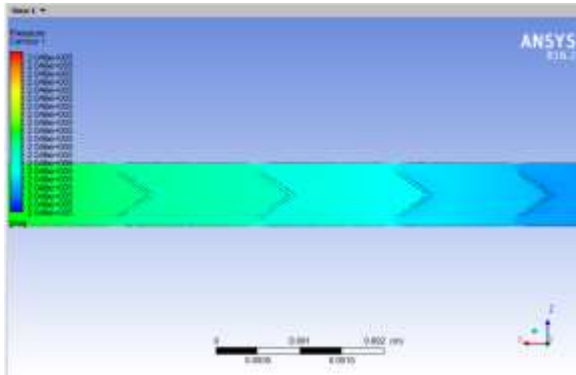
The governing equations of the problem were solved, numerically, using a control volume method, and finite element volume (FEV) used in order to calculate the thermo physical properties. As a result of a grid independence study, a grid size of 1200 x 1024 was found to model accurately the flow fields described in the corresponding results.

The accuracy of the computer model was verified by comparing results from the present study with those obtained by Gongnan [11] turbine duct heat transfer.

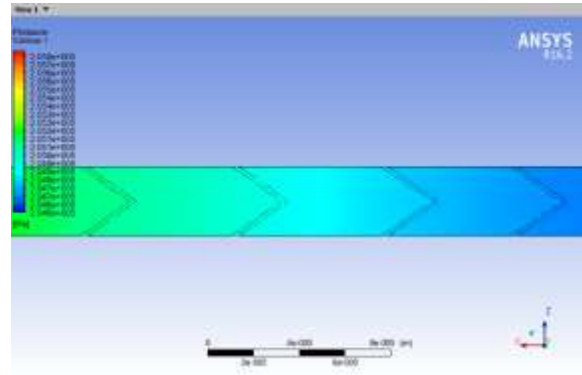
Table 1 Validation of Nusselt number and Pressure drop

<b>Continuous ribs Ref. [11]</b>				
	<b>2Mesh</b>	<b>2.5Mesh</b>	<b>3.5Mesh</b>	<b>4Mesh</b>
<b>Nu</b>	108.394	109.439	109.788	109.631
<b><math>\Delta p</math></b>	91.887	92.104	92.082	92.083
<b>V-Shape Continuous ribs with 35-deg (Present FEV (ANSYS))</b>				
<b>Nu</b>	90.78	91.298	91.567	91.892
<b><math>\Delta p</math></b>	78.58	78.56	78.88	78.95
<b>Truncated ribs Ref. [11]</b>				
<b>Nu</b>	98.653	99.611	100.275	100.274
<b><math>\Delta p</math></b>	83.735	83.986	84.021	84.019

V-Shape Truncated ribs with 35-deg (Present FEV (ANSYS))				
<b>Nu</b>	87.65	87.588	87.785	87.658
<b><math>\Delta p</math></b>	83.735	83.986	84.021	84.019

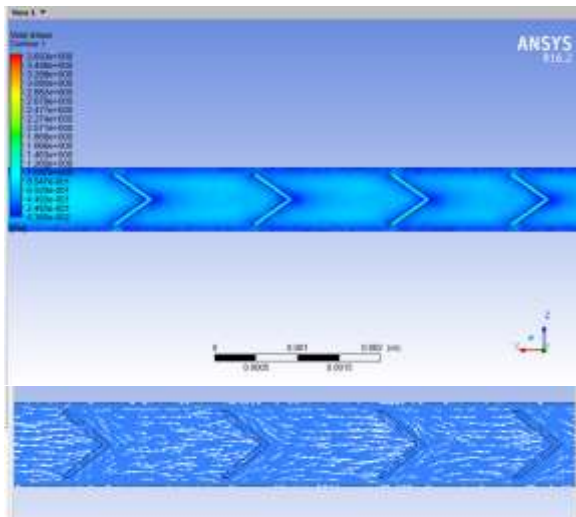


(a)

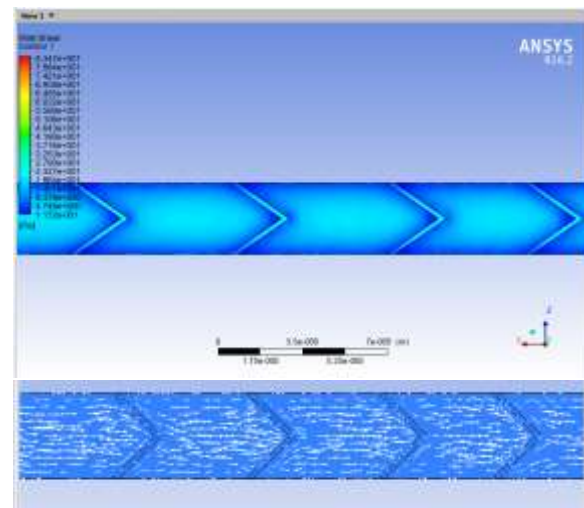


(b)

Figure 5.1 (a) Pressure contours in V-shape 35-deg truncated ribs duct and (b) Pressure contours in V-shape 35-deg Continuous ribs duct

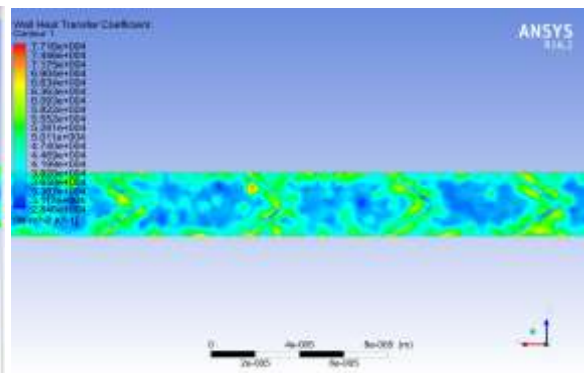
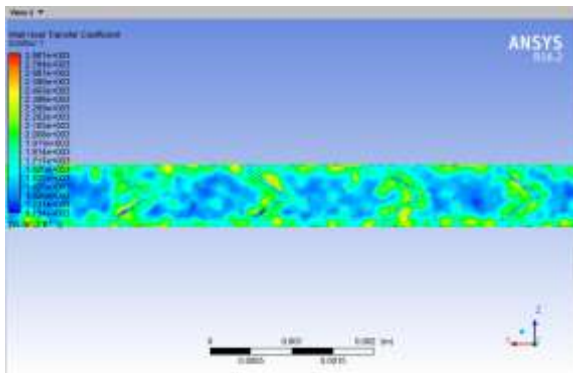


(a)



(b)

Figure 5.2 (a) and (b) Wall shear stress in V-shape 35-deg truncated and Continuous ribs duct



(a) (b)  
Figure 5.3 (a) and (b) Wall Heat transfer coefficient in V-shape 35-deg truncated and Continuous ribs duct

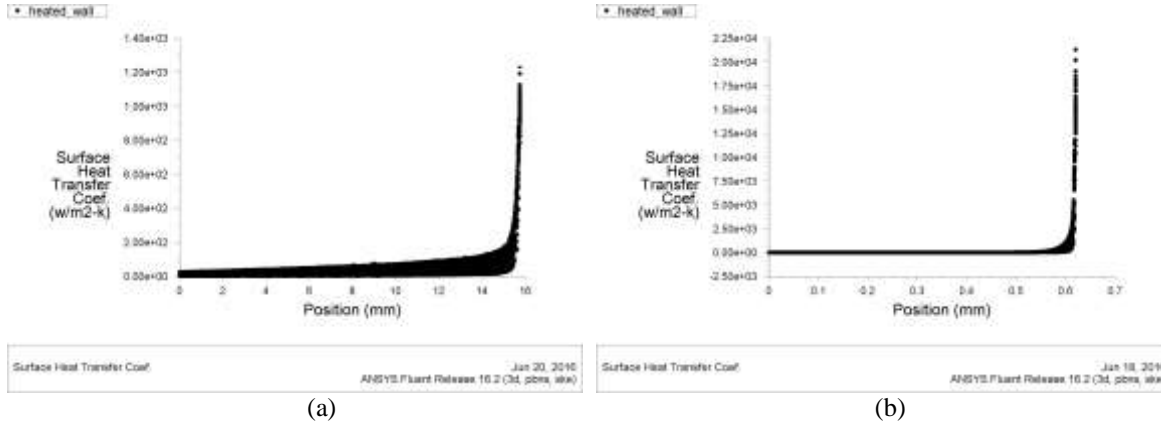


Figure 5.4 (a) and (b) Surface Heat transfer coefficient in V-shape 35-deg truncated and Continuous ribs duct

Table 2 Friction Factor Comparison between Truncated and Continuous Ribs and V-shape 35-deg Truncated and Continuous ribs

S.No	Reynolds Number, Re	Truncated Ribs [11]	Continuous Ribs [11]	Truncated Ribs V-shape 35-deg (present)	Continuous Ribs V-shape 35-deg (present)
1	20000	3.536	3.271	3.752	3.578
2	40000	4.172	3.794	4.459	4.256
3	60000	4.607	4.197	4.956	4.769

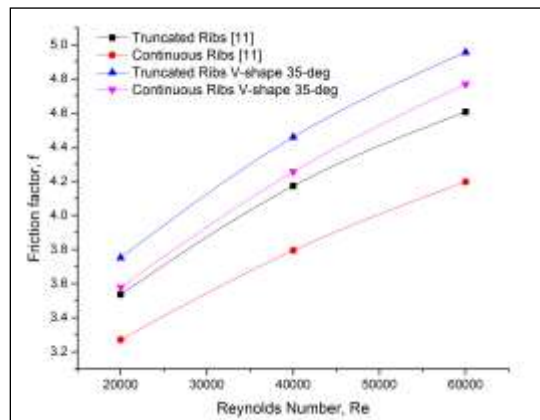


Figure 5.5 Variation of friction factor in different Ribs

Figure 5.5 and table 1 shows the variation effect of friction factor in Truncated, Continuous Ribs [11] and V-shape 35-deg Truncated and Continuous ribs (present ANSYS result). It is observing that friction factor increases as Reynolds number increases. However, the friction factor in V-shape 35-deg truncated ribs is more as compared to continuous ribs.

It can also be concluding that the friction factor in truncated ribs 8%-9% is more as compared to other ribs.

Table 3 Nusselt Number comparison in different ribs

S.No	Reynolds Number, Re	Truncated Ribs [11]	Continuous Ribs [11]	Truncated Ribs V-shape 35-deg (present)	Continuous Ribs V-shape 35-deg (present)
1	20000	47.58	44	57.68	55.689
2	40000	74.82	68.37	85.658	81.658
3	60000	106.7	96.33	110.36	98.975

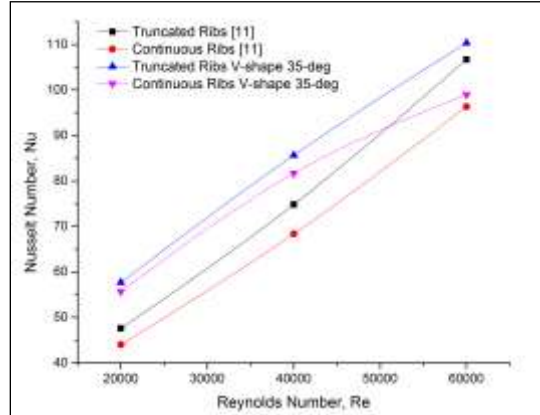


Figure 5.6 Variation of Nusselt Number in different ribs configuration

Figure 5.6 and table 6.3 shows the variation of Nusselt Number in different ribs configuration. It can be concluding that the sidewall Nusselt numbers of the channel or duct in V-shape 35-deg truncated ribs configuration is more as compared to other ribs. The Nusselt number linearly goes on increasing as the flow increases.

It can also be configured that Nusselt number of truncated ribs is more as compared to other ribs. Whereas approx. 40.2% as compared to other ribs, so that the overall heat transfer is more in truncated ribs are compared to other.

Table 4 Comparative Heat transfer and pressure drop in ribs

S.No	Reynolds Number, Re	Truncated Ribs [11]	Continuous Ribs [11]	Truncated Ribs V-shape 35-deg (present)	Continuous Ribs V-shape 35-deg (present)
1	20000	35.62	40.18	22.54	35.95
2	40000	187.2	210	96.47	152.358
3	60000	333.3	366.2	285.68	304.658

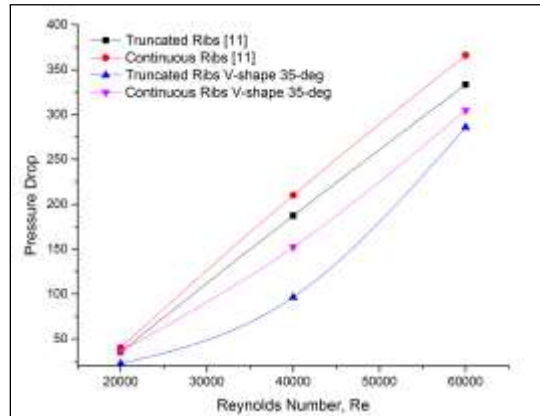


Figure 5.7 Variation of Heat transfer and pressure drop in different ribs

Figure 5.7 and Table 6.4 shows the Comparative pressure drop in ribs. It has been scrutinized that the on increasing Reynolds number pressure drop goes on increasing.

Initially the pressure of both the ribs are same but as the Reynolds number increases the variation in pressure drop within the channel is seen and the pressure drop is more significant in V-shape 35-deg truncated ribs as compared with others ribs.

Table 5 Heat transfer coefficient in different ribs

S.No	Reynolds Number, Re	Truncated Ribs [11]	Continuous Ribs [11]	Truncated Ribs V-shape 35-deg (present)	Continuous Ribs V-shape 35-deg (present)
1	20000	37.07	35.21	45.78	39.457
2	40000	82.24	77.29	85.65	81.65
3	60000	147.5	136.4	155.658	145.98

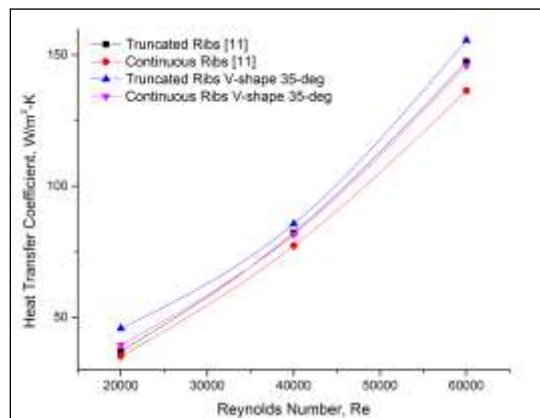


Figure 5.8 Variation of Heat transfer coefficient in different ribs

Figure 5.8 and table 5 shows Variation of Heat transfer coefficient with in different ribs for the channels with different ribs configuration. It has been observed that all the rib configuration has similar trend. Both the Heat transfer coefficient is monotonous for continuous ribs. Therefore, the side-wall with both continuous ribs facilitates good performance for improving gas turbine blade cooling at the same pumping power.

**CONCLUSION AND FUTURE SCOPE**

Computational Simulation of turbine blade cooling duct has been carried out and the heat transfer with the ribs are evaluated as well as compared and several conclusions are drawn

- The Nusselt number of V-shaped 35-deg truncated ribs is more as compared to normal truncated and both continuous ribs. Whereas compared to normal truncated and both continuous ribs, so that the overall heat transfer is more in V-shape 35-deg truncated ribs are compared to other.
- Heat Transfer Augmentation Quantity of continuous ribs is more as compared with other ribs.
- The Flow structure near leading edge can be improved by implementing V-shaped 35-deg Truncated rib.
- Also the heat transfer of the side will also increases by using V-shaped 35-deg truncated ribs.
- The heat transfer coefficient is more in V-shaped 35-deg truncated as compared to others.
- On increasing Reynolds number heat transfer significantly increases.
- The parametric ratio such as length affects the heat transfer of ribs along with friction characteristics.
- In both continuous ribs side wall thermal performance is higher along with friction factors when compared with V-shaped 35-deg truncated ribs only when pressure loss of passage taken in consideration.

**Future Scope**

- Different shape and size of ribs can be analyzed.
- Boundary layer separation can also be considered
- Presence of heat flux and thermal loss at different turbulence model can be compared.
- Thermodynamic analysis of duct can be done i.e exergy analysis.

**REFERENCE**

- [1] H. Iacovides, B.E. Launder, "Computational fluid dynamics applied to internal gas-turbine blade cooling: a review Review Article", International Journal of Heat and Fluid Flow, Volume 16, Issue 6, December 1995, Pages 454-470
- [2] Srinath V. Ekkad, Je-Chin Han "Detailed heat transfer distributions in two-pass square channels with rib turbulators", International Journal of Heat and Mass Transfer, Volume 40, Issue 11, July 1997, Pages 2525-2537
- [3] Mahfoud Kadja\* and George Bergelest, "Computational Study Of Turbine Blade Cooling By Slot-Injection Of A Gas", Applied Thermal Engineering Vol. 17, No. 12. pp. 1141-1149. 1997
- [4] A.B Smith, A Kempster, J Smith, "Vapour aluminate coating of internal cooling channels, in turbine blades and vanes", Surface and Coatings Technology, Volumes 120-121, November 1999, Pages 112-117
- [5] Akira Murata, Sadanari Mochizuki, "Large eddy simulation with a dynamic subgrid-scale model of turbulent heat transfer in an orthogonally rotating rectangular duct with transverse rib turbulators", International Journal of Heat and Mass Transfer, Volume 43, Issue 7, April 2000, Pages 1243-1259
- [6] A. Ooi, G. Iaccarino, P.A. Durbin, M. Behnia, "Reynolds averaged simulation of flow and heat transfer in ribbed ducts", International Journal of Heat and Fluid Flow, Volume 23, Issue 6, December 2002, Pages 750-757
- [7] P.R. Chandra, C.R. Alexander, J.C. Han, "Heat transfer and friction behaviors in rectangular channels with varying number of ribbed walls", International Journal of Heat and Mass Transfer, Volume 46, Issue 3, January 2003, Pages 481-495
- [8] Mohammad H. Albeirutty, Abdullah S. Alghamdi, Yousef S. Najjar, "Heat transfer analysis for a multistage gas turbine using different blade-cooling schemes", Applied Thermal Engineering, Volume 24, Issue 4, March 2004, Pages 563-577
- [9] D.K. Tafti, "Evaluating the role of subgrid stress modeling in a ribbed duct for the internal cooling of turbine blades", International Journal of Heat and Fluid Flow Volume 26, Issue 1, February 2005, Pages 92-104
- [10] Neil Zuckerman, Noam Lior, "Impingement Heat Transfer: Correlations and Numerical Modeling", 544 *Ö* Vol. 127, MAY 2005 Copyright © 2005 by ASME Transactions of the ASME
- [11] Gongnan Xie, Weihong Zhang, Bengt Sunden, "Computational analysis of the influences of guide ribs/vanes on enhanced heat transfer of a turbine blade tip-wall", International Journal of Thermal Sciences 51 (2012)

- [12] Evan A. Sewall, Danesh K. Tafti, Andrew B. Graham, Karen A. Thole, "Experimental validation of large eddy simulations of flow and heat transfer in a stationary ribbed duct", *International Journal of Heat and Fluid Flow*, Volume 27, Issue 2, April 2006, Pages 243-258
- [13] André Burdet, Reza S. Abhari, Martin G. Rose "Modeling of Film Cooling—Part II: Model for Use in Three-Dimensional Computational Fluid Dynamics", *Journal of Turbomachinery* Copyright © 2007 by ASME APRIL 2007, Vol. 129 / 221
- [14] R. Kamali, A.R. Binesh, "The importance of rib shape effects on the local heat transfer and flow friction characteristics of square ducts with ribbed internal surfaces", *International Communications in Heat and Mass Transfer*, Volume 35, Issue 8, October 2008, Pages 1032-1040
- [15] Shyy Woei Chang, Tsun Lirng Yang, Tong-Miin Liou, Guo Fang Hong, "Heat transfer of rotating rectangular duct with compound scaled roughness and V-ribs at high rotation numbers", *International Journal of Thermal Sciences* 48 (2009) 174–187
- [16] Kyung Min Kim, Jun Su Park, Dong Hyun Lee, Tack Woon Lee, Hyung Hee Cho, "Analysis of conjugated heat transfer, stress and failure in a gas turbine blade with circular cooling passages", *Engineering Failure Analysis*, Volume 18, Issue 4, June 2011, Pages 1212-1222
- [17] Pongjet Promvonge, Wayo Changcharoen, Sutapat Kwankaomeng, Chinaruk Thianpong, "Numerical heat transfer study of turbulent square-duct flow through inline V-shaped discrete ribs", *International Communications in Heat and Mass Transfer* 38 (2011) 1392–1399
- [18] N.M. Yusop, A.H. Ali, M.Z. Abdullah, "Validation of three dimensional film cooling modeling on convex surface for gas turbine blade", *International Communications in Heat and Mass Transfer* 39 (2012) 830–837.
- [19] Wang, L., and Sunden, B, "Experimental Investigation of Local Heat Transfer in a Square Duct with Continuous and Truncated Ribs," *Exp. Heat Transfer*, 18, pp. 179–197, 2005
- [20] Abhishek G. Ramgadia, Arun K. Saha, "Three-dimensional numerical study of turbulent flow and heat transfer in a wavy-walled duct", *International Journal of Heat and Mass Transfer* 67 (2013) 98–117
- [21] Gongnan Xie, Shian Li, Weihong Zhang, "Computational Fluid Dynamics Modeling Flow Field and Side-Wall Heat Transfer in Rectangular Rib-Roughened Passages", *Journal of Energy Resources Technology* Copyright VC 2013 by ASME DECEMBER 2013, Vol. 135 / 042001-1
- [22] O. Labbé, "Large-eddy-simulation of flow and heat transfer in a ribbed duct", *Computers & Fluids* 76 (2013) 23–32.
- [23] Linqi Shui, Jianmin Gao, Xiaojun Shi, Jiazeng Liu, "Effect of duct aspect ratio on heat transfer and friction in steam-cooled ducts with 60° angled rib turbulators", *Experimental Thermal and Fluid Science* 49 (2013) 123–134
- [24] Eun Yeong Choi, Yong Duck Choi, Won Suk Lee, Jin Teak Chung, Jae Su Kwak, "Heat transfer augmentation using a ribedimple compound cooling technique", *Applied Thermal Engineering* 51 (2013) 435e441
- [25] K. Elebiary M. E. Taslim, "Experimental/Numerical Crossover Jet Impingement in an Airfoil Leading-Edge Cooling Channel", *Journal of Turbo machinery* Copyright VC 2013 by ASME JANUARY 2013, Vol. 135 / 011037-1
- [26] Sukhjinder Singh, Danesh Tafti, Colin Reagle, Jacob Delimont, Wing Ng, Srinath Ekkad, "Sand transport in a two pass internal cooling duct with rib turbulators" *International Journal of Heat and Fluid Flow* Volume 46, April 2014, Pages 158–167
- [27] Matteo Pascotto, Alessandro Armellini, Claudio Mucignat, "Coriolis Effects on the Flow Field Inside a Rotating Triangular Channel for Leading Edge Cooling", *Journal of Turbomachinery* Copyright VC 2014 by ASME MARCH 2014, Vol. 136 / 031019-1